https://doi.org/10.46813/2025-155-084

DISSOCIATION OF OXYGEN AND WATER MOLECULES IN NEGATIVE CORONA

B.B. Kadolin, I.N. Onishchenko, V.M. Ostroushko, G.V. Taran

National Science Center "Kharkiv Institute of Physics and Technology", Kharkiv, Ukraine

E-mail: ostroushko-v@kipt.kharkov.ua

Numerical simulations of negative corona in the Trichel pulse mode with calculations of dissociation rates of oxygen molecules in air and oxygen and of water molecules in humid air are carried out. It is found that the yield of oxygen atoms and hydroxyl radicals from the first pulse is considerably greater than from each of subsequent pulses and the main part of dissociation acts occurs during the ionization wave propagation over the cathode surface in a small space of intensive impact ionization. The obtained differences in ratio of dissociation rates at the different stages of ionization wave propagation and for different subsequent pulses are explained by the difference in the characteristics of the ionization wave at these stages and pulses, determined by different dependences of the frequencies of electron processes on the field strength.

PACS: 52.80.Hc

INTRODUCTION

Negative corona in oxygen-containing gases can be an effective source of ozone, and in the presence of water vapor, hydroxyl radicals are formed. If a constant voltage of a specific level is applied to the gap filled with gas, containing electronegative components, then the negative corona is realized in the form of a quasi-periodic process (Trichel pulses).

There are a lot of works (in particular, [1–6]), in which experimental research and numerical simulations of Trichel pulses have been carried out. In them, in the simulations, the evolution of the spatial distribution of charged particles over time was obtained. In the present work, the simulations include the calculations of evolution of the oxygen and water molecule dissociation intensity in space over time.

STATE OF PROBLEM

Simulations were performed under the assumption of axial symmetry of the processes, for an axially symmetric discharge gap with electrodes in the form of hyperboloids of revolution. A curvature radius of the cathode tip was about 50 μm. An anode was concave from the side of the gap and the curvature radius of its tip was large. The charged particle densities evolution was determined with taking into account the processes of drift, diffusion, ionization, attachment, and recombination, ion-ion and electron-ion one. The equations describing the evolution are given in [7]. Each given voltage value was applied instantaneously. To combine the requirement of a small step of time integration during the rapid development of ionization flashes and the need to simulate several pulses, it was used a variable time step. It was changed so that the maximum value of relative change of the particle densities over the discharge gap at one time step was approximately kept at a certain level. To start ionization, it was assumed nonzero initial electron density in the gap. For sufficiently small its value, its further decrease has almost no effect on the characteristics of pulses, only the time of the first pulse development increases.

The following four electronic processes make a significant contribution to the dissociation of oxygen:

$$O_2 + e \rightarrow O + O + e,\ O_2 + e \rightarrow O + O(^1D) + e,$$

$$O_2 + e \rightarrow O + O^-,\ O_2 + e \rightarrow O + O^+ + e + e,$$

and the main contribution is given by those two of them, in which the number of free electrons does not change. Similarly, from two processes, $H_2O + e \rightarrow H + OH + e$ and $H_2O + e \rightarrow H + OH^-$, which give a significant contribution to the dissociation of water, the main contribution is given by the first one. The dependences of the constants of these processes on the electric field strength were obtained with use of BOLSIG+ code [10] and the cross sections given in [8, 9].

The formation of hydroxyl radicals was considered for the air with low humidity, when the presence of water vapor nearly does not affect the time evolution of electron distribution in space, and so, the rate of OH radical production is approximately proportional to the water vapor density. For certainty, results are given for 1% mole fraction of water vapor (dew point about 7 °C).

The pulse sequency become periodical gradually, and the characteristics of the first pulse differ significantly from the characteristics of subsequent pulses. The productivity of any process may be characterized by an overall number of its acts carried out in the entire discharge gap up to the current time instant from the beginning. The time derivative of such quantity is the overall intensity of the corresponding process in the gap. The productivity of the pulses with respect to the given process may be characterized by the change of the mentioned quantity over time between the corresponding local minima of its time derivative. The simulations were carried out for the discharge in air at atmospheric pressure, in air of elevated pressure and in oxygen. For the discharge in air at elevated pressure, it was used the similarity of gas discharge processes at the fixed values of the product of pressure on the characteristic size of the electrode system and the ratio of the mentioned product with the applied voltage.

The electron free path between successive acts of impact ionization, $e + O_2 \rightarrow e + e + O_2^+$, or dissociative attachment, $e + O_2 \rightarrow O^- + O$, is inversely proportional to the pressure, and the free path between the acts of three-body attachment, $e + O_2 + M \rightarrow O_2^- + M$, is inversely proportional to the square of the pressure, which violates the described similarity. Also, the similarity may be violated due to a change in the temperature regime, through a decrease of the heat removal possibility when the dimensions are reduced. In the simulations related to elevated pressure, the parameters of the gas differed from the parameters of atmospheric air only by multiplying the three-body attachment constant on a value identical for all field strengths. In the simulations of the discharge in oxygen, the only parameter that distinguished the gas from atmospheric air was an attachment frequency 5 times greater for all field strength values.

SIMULATION RESULTS

As it is known, each cycle of Trichel pulses begins with formation of the plasma space in the discharge gap in the vicinity of the cathode and its subsequent propagation towards the cathode as an ionization wave. The ionization wave propagation towards the cathode can change into its propagation over the cathode surface. Then the ionization processes are dumped, due to the negative ion cloud formation at some distance from the cathode leading to a decrease of the field near the cathode.

Simulations of the discharge in atmospheric air carried out for different values of the applied voltage showed that the overall numbers of dissociation acts in the first pulse are significantly greater than ones in the subsequent pulses. The smallest number of dissociation acts occurs during the second pulse, and each next pulse is characterized by the dissociation acts number increase, with a decrease of that increase at the next pulse. A decrease in the applied voltage value leads to a decrease of the dissociation act number in each pulse, and the ratio of the numbers of the dissociation acts at the first pulse and at the certain subsequent pulse decreases. It is so, because at the smaller voltage value it is sufficient the smaller number of negative ions to weaken the field and to stop the first pulse development, and the conditions for development of subsequent pulses approach ones for the first pulse. When the voltage approaches the lower threshold of the Trichel pulse mode, the sensitivity of the dissociation act number at each pulse to the change in voltage increases significantly, the time interval between pulses increases and the peak values of the total current and the number of dissociation acts during the first and subsequent pulses converge, because the possibility of development of each subsequent pulse at such voltage level requires almost complete cleaning of the discharge gap from negative ions, with the gap content approaching the content before the first pulse.

In the discharge simulations in high-pressure air, the enhancement of three-body attachment leads to a decrease in the peak values of the total current and the intensity of dissociation during pulses, at the fixed applied voltage value. This is also the case for any attachment enhancement. But intensity of three-body attachment is large at the small field strength, and its enhancement contributes to the formation of negative ions in a significant part of discharge gap, and not only during ionization flashes, but also during the time interval between them. And a larger charge of negative ions weakens the field during the development of the next pulse more and stops the increase of the total current at a smaller value. For the subsequent pulses, the dissociation intensity decrease with the enhancement of three-body attachment is relatively stronger compared to the first pulse, because of greater sensitivity of the process to the field weakening in the weaker field. And for discharge in oxygen, the same reason gave considerably larger values of the ratios of the dissociation act numbers during the first and subsequent pulses, than for discharge in air.

In the humid air, the water dissociation rate is more sensitive to the field weakening, than the oxygen dissociation rate, due to nearly 1.5 times greater energy threshold of the process, and the obtained ratios of the production during the first and subsequent pulses for hydroxyl radicals were significantly greater than ones for atomic oxygen.

In Fig. 1 there are shown the time dependences for the quantities $y = (x - x_0) / (x_1 - x_0)$, where x denotes, respectively, the total current (tct), the maximum value of the electric field strength in the gap (efs), the overall amount of electrons (eln) or positive ions (pin) in the gap, the overall rate of the process of ionization (inz), attachment (att), or dissociation, with the formation of hydroxyl radicals (OH) or atomic oxygen (O), or the ratio of those rates (OH:O), and the ranges $x_0 \ldots x_1$ of x quantities, corresponding to the 0…1 range of y quantity, for the mentioned discharge characteristics are, respectively, as follows: $((3 \cdot 10^{-5} \ldots (2.35 \cdot 10^{-3}))$ A (tct), $(5.5 \cdot 10^5 \ldots 1.6 \cdot 10^6)$ V / cm (efs), $(3.1 \cdot 10^6 \ldots 3.0 \cdot 10^8)$ (eln), $(4 \cdot 10^6 \ldots 3.54 \cdot 10^8)$ (pin), $(1.3 \cdot 10^{15} \ldots 7.2 \cdot 10^{16})$ s^{-1} (inz), $(4 \cdot 10^{14} \ldots 2.2 \cdot 10^{16})$ s^{-1} (att), $(8 \cdot 10^{13} \ldots 1.8 \cdot 10^{15})$ s^{-1} (OH), $(3 \cdot 10^{16} \ldots 9.3 \cdot 10^{17})$ s^{-1} (O), $(0 \ldots 3.3 \cdot 10^{-3})$ (OH:O).

In Fig. 2, for three instants, it is shown the distribution of the electrons and positive ion densities, of the quantity $-E^{-1}$, determined by the electric field strength E, and of the volumetric intensities of hydroxyl radical and oxygen atom production near the cathode.

The simulations showed that the main part of the dissociation acts (see Fig. 1,a, two last rows in Fig. 2) take place at the second stage of the ionization wave propagation, over the cathode surface, in the small space of intensive impact ionization, in front of the plasma space which the wave leaves behind during its propagation. And the ratio of oxygen atom and hydroxyl radical production rates at this stage of pulse development changes with time weakly (see Fig. 1,a). A considerable contribution to dissociation is also given by the first stage of the ionization wave propagation, towards the cathode. Its duration is relatively small and at this stage the conditions for the formation of hydroxyl radicals are relatively more favorable (see Fig. 1,a). The transition between the specified stages of ionization wave propagation occurs mainly after the time instant

corresponding to the local minimum of the total current between its local maxima, and the left column in Fig. 2 approximately corresponds to the time of beginning of the transition.

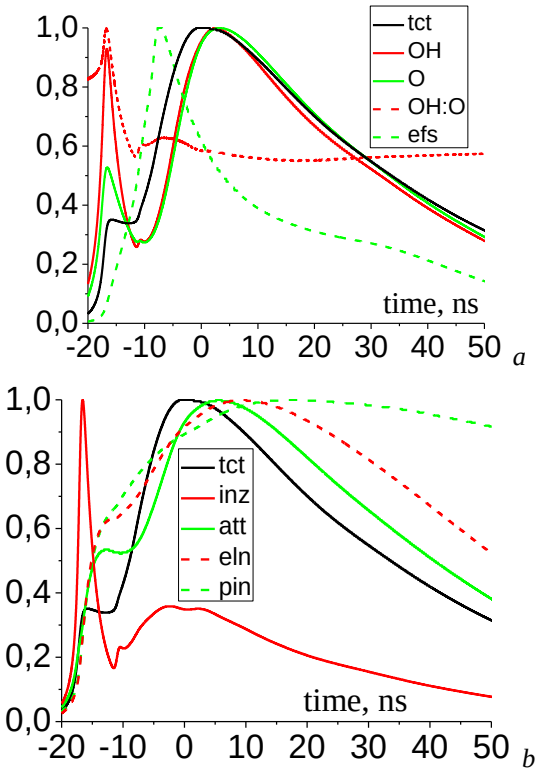

Fig. 1. The dependences of the normalized quantities corresponding to the total current (tct), the maximum value of the electric field strength (efs), the overall number of electrons (eln) and positive ions (pin) in the gap and the overall rates of ionization (inz), attachment (att) and dissociation, with the formation of hydroxyl radicals (OH) and oxygen atoms (O), and the ratio of the rates (OH:O), on the time taken relative to the instant of the total current maximum

The change of the ratio between the rates of production of oxygen atoms and hydroxyl radicals during the ionization wave propagation over the cathode surface is small. It is so, because the main part of dissociation acts in ionization waves occur at the end of the zone of intensive ionization, in front of the plasma space. There, in the process of avalanche multiplication of electrons, the electron density (see the first row in Fig. 2) approached the maximum value, at which the field relaxation time, determined by a medium conductivity, decreases to the time of the order of time between successive ionization acts carried out by one electron during its motion, but the field relaxation has not yet occurred. Then the field strength values (see the third row in Fig. 2) are still large and they belong to the interval, in which the values of the constants of the oxygen and water dissociation processes depend on the strength value weakly. And as the volumetric intensities of the considered dissociation processes are equal to the products of electron density on the constants of the processes and the processes are localized in a small space, the ratio of the overall rates of oxygen and water dissociation processes is determined by the field strength level in that space.In the ionization wave directed towards the cathode (see with the distributions close to those shown in the left column of Fig. 2), the field strength in space at the end of the intensive ionization zone is greater than one in the wave propagating over the cathode surface. It is due to somewhat different conditions of these waves' propagation. During the propagation of the ionization wave over the cathode surface, there is an intensive emission of electrons from the cathode, due to a powerful flow of positive ions to the cathode surface (see Fig. 1,b, the second row in Fig. 2), thanks to which, to achieve such value of electron density, at which field relaxation occurs, a smaller number of successive acts of electron multiplication in avalanches is enough, and it can be achieved at a field strength less than that characteristic for an ionization wave propagating towards the cathode. The ratio of the overall rates of hydroxyl radical and atomic oxygen production is determined by the field strength level in a small space with intensive dissociation, and the dissociation constant for hydroxyl radical is more sensitive to the field strength decrease than one for atomic oxygen, due to the higher energy threshold of the water dissociation process. As a result, the ratio of the overall rates of hydroxyl radical and atomic oxygen production in the ionization wave propagating over the cathode surface is less than one in the ionization wave directed towards the cathode (see Fig. 1,a). And the ratio of overall rates for the ionization process (see Fig. 1,b) at the stages of ionization wave propagation towards the cathode and over the cathode surface is greater than one for hydroxyl radical production (see Fig. 1,a), due to the higher energy threshold of the process.

In the simulations, the second and subsequent ionization flashes developed from the remnants of the destruction of that part of the plasma space that was formed at the end of the ionization wave propagation over the cathode surface, so, according to the axial symmetry embedded into the model, the flashes in space had the shape of a ring. It is obvious that in an axially symmetric electrode system, but without imposing axial symmetry on the processes, such flashes are unstable with respect to disturbances, in which, in some azimuthal sector, the avalanches develop faster, the plasma space forms and propagates earlier, and then the ionization begins to fade anywhere. Through such azimuthal instability, the characteristics of the second and subsequent Trichel pulses, obtained in axially symmetric simulations, may correspond to the real ones only by an order of magnitude.

But the axially symmetric propagation of the ionization wave over the cathode surface seems to be stable with respect to branching into several "streamers" that would propagate in different radial directions. Such conclusion is based on the presented in [11] consideration of a certain simplified two-dimensional model of the development of electron avalanches outside of a positively charged perfectly conducting surface, which is uniform in the axial direction and has a small sinusoidal variation of the shape by the azimuthal angle, in cylindrical coordinates.

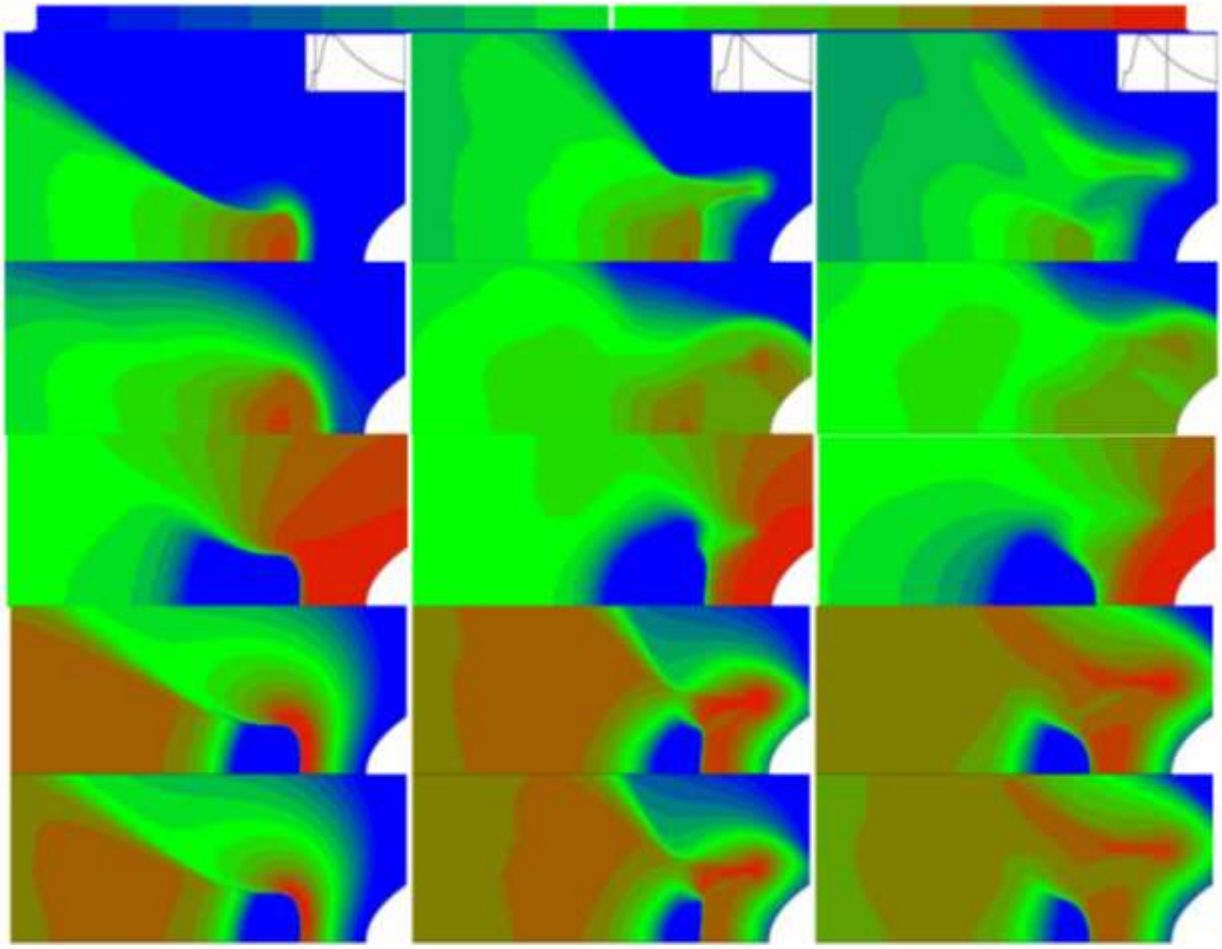

Fig. 2. Time evolution (three consecutive columns, from left to right, respectively, correspond to three instants with an interval of 20 ns) of distribution of electron and positive ion densities, of the quantity $-E^{-1}$, determined by the electric field strength E, and of the volumetric intensities of hydroxyl radicals and oxygen atoms production (five consecutive rows, from the top down, respectively) in a space 0.5 mm wide, with the white tip of the cathode in the lower right corner. The color scale (16 colors above the figure) is linear for the quantity $-E^{-1}$, and logarithmic for other quantities. For both densities, for field strengths, and for volumetric intensities of hydroxyl radical and oxygen atom production, the "maximum blue" color refers to values less than $10^{9+(3/8)}$ cm^{-3}, $(4/3)\cdot10^{4}$ V/cm, $10^{9+(3/4)}$ cm$^{-3}\cdot$s^{-1}, and $10^{12+(3/4)}$ cm$^{-3}\cdot$s^{-1}, and "maximum red" color refers to values greater than $10^{15-(3/8)}$ cm^{-3}, $2\cdot10^{5}$ V/cm, $10^{21-(3/4)}$ cm$^{-3}\cdot$s^{-1}, and $10^{24-(3/4)}$ cm$^{-3}\cdot$s^{-1}, respectively. In the upper right corners of the first row, the time dependence of the total current is shown, with a vertical line, for the time instant corresponding to the given column

One of the methods of increasing the efficiency of plasma chemical reactors is pulsed voltage application [12], which brings the characteristics of the discharge closer to the characteristics of the pulse, which is the first in the sequence of those that develop when the voltage value does not change after application. The expediency of the pulse power use increases when the first pulse produces significantly more active particles than subsequent pulses. Therefore, in accordance with the above, for the atomic oxygen production in oxygen or in air at the elevated pressure or for the hydroxyl radical production in humid air at atmospheric pressure, the use a pulse voltage instead of a constant one not very close to the lower threshold of the Trichel pulse mode is more expedient, than its use for atomic oxygen production in air at atmospheric pressure. On the other hand, the approach of the constant voltage to the lower threshold of the Trichel pulse mode leads to a decrease in the average rate of active particles production roughly proportional to the decrease in the frequency of pulses, and therefore the use of discharge with so low constant voltage for active particles production is hardly advisable.

CONCLUSIONS

By the numerical simulations of the atomic oxygen and hydroxyl radical production in the Trichel pulse mode of the negative corona it is found that the main part of dissociation acts takes place in the small space of intensive impact ionization during the ionization wave propagation over the cathode surface, and the time variation of the ratio of the overall production rates of oxygen atoms and hydroxyl radicals during the mentioned propagation is weak. The obtained differences in ratio of dissociation rates at the different stages of ionization wave propagation and for the different subsequent pulses are explained through the difference of the wave characteristics at these stages and

pulses determined by different dependences of the frequencies of electron processes on the field strength. It is found that the yields of oxygen atoms and hydroxyl radicals during the first pulse are significantly more than ones during each of the subsequent pulses, which makes it expedient to use a pulse power supply instead of a constant voltage, to increase the efficiency of production of the mentioned active particles.

REFERENCES

1. G.W. Trichel. The mechanism of the negative point to plane corona near onset // *Physical Review*. 1938, v. 54, No.12, p. 1078-1084.
2. R. Morrow. Theory of negative corona in oxygen // *Physical Review A*. 1985, v. 32, No. 3, p. 1799-1809.
3. M. Černák, T. Hosokawa, S. Kobayashi, and T. Kaneda. Streamer mechanism for negative corona current pulses // *Journal of Applied Physics*. 1998, v. 83, No.11, p. 5678-5690.
4. R. Morrow. Theory of stepped pulses in negative corona discharges // *Physical Review A.* 1985, v. 32, No.6, p.3821-3824.
5. A.P. Napartovich, Yu.S. Akishev, A.A. Deryugin, I.V. Kochetov, M.V. Pan'kin, N.I. Trushkin. A numerical simulation of Trichel pulse formation in a negative corona // *Journal of Physics D: Applied Physics*. 1997, v. 30, p. 2726-2736.
6. Yu.S. Akishev, I.V. Kochetov, A.I. Loboiko, A.P. Napartovich. Numerical simulations of Trichel pulses in a negative corona in air // *Plasma Physics Reports*. 2002, v. 28, No.12, p. 1049-1059.
7. O. Bolotov, B. Kadolin, S. Mankovskyi, I. Pashchenko, O. Poliakov, G Taran, L. Zavada, V. Ostroushko. Numerical simulations of quasi-stationary streamer propagation // *Problems of Atomic Science and Technology*. 2016, No. 5 (105), p. 121-125.
8. P.C. Cosby. Electron-impact dissociation of oxygen // *Journal of Chemical Physics*. 1993, v. 98, p. 9560-9569.
9. Mi-Young Song et al. Cross sections for electron collisions with H_2O // *Journal of Physical Chemistry Reference Data*. 2021, v. 50, p. 023103.
10. G.J.M. Hagelaar and L.C. Pitchford. Solving the Boltzmann equation to obtain electron transport coefficients and rate coefficients for fluid models // *Plasma Sources Sci. Technology*. 2005, v. 14, p. 722-733.
11. V. Ostroushko. Numerical simulation of reproduction of the development conditions of the next Trichel pulse in negative corona // *Problems of Atomic Science and Technology*. 2023, No. 4(146), p. 134-138.
12. G.V. Taran, B.B. Kadolin, V.M. Ostroushko, I.A. Paschenko. Study of the dependence of the characteristics of the pulse negative corona on the parameters of the combined high voltage power supply // *Problems of Atomic Science and Technology*. 2023, No. 4(146), p. 160-163.

Article received 01.11.2024
Article accepted 17.01.2025

ДИСОЦІАЦІЯ МОЛЕКУЛ КИСНЮ ТА ВОДИ У НЕГАТИВНІЙ КОРОНІ

Б.Б. Кадолін, І.М. Оніщенко, В.М. Остроушко, Г.В. Таран

Виконане числове моделювання негативної корони у режимі імпульсів Тричела з розрахунком темпів дисоціації молекул кисню у повітрі, та кисню і молекул води у вологому повітрі. Виявлено, що утворення атомарного кисню та гідроксильних радикалів у першому імпульсі є значно більшим, ніж у кожному з наступних імпульсів, і основна частина актів дисоціації відбувається під час поширення хвилі іонізації над поверхнею катода у малому просторі інтенсивної ударної іонізації. Отримані відмінності співвідношення темпів дисоціації на різних стадіях поширення хвилі іонізації та для різних послідовних імпульсів пояснені як результат відмінностей характеристик хвилі іонізації для вказаних стадій та імпульсів, визначених різною залежністю частот електронних процесів від напруженості поля.